# Population kinetics of lithiumlike and berylliumlike ions in low temperature dense recombining plasma

Tetsuya Kawachi
*Advanced Photon Research Center, Japan Atomic Energy Research Institute (JAERI), 8-1 Umemidai, Kizu, Soraku, Kyoto 619-0215, Japan*
(Received 24 September 2002; published 29 January 2003)

A collisional-radiative model for the lithiumlike and berylliumlike ions has been constructed. In this model, virtually all the doubly excited levels of the berylliumlike ions are taken into account. Time-differential coupled rate equations for the level populations of the lithiumlike and berylliumlike ions are solved under a recombining plasma condition, and the population kinetics of these ions, especially for the validity of quasi-steady state (QSS) approximation and the population flux into and out of excited levels, is discussed. Temporal evolution of gains of the $3d\,^2D$-$4f\,^2F$ and $3d\,^2D$-$5f\,^2F$ lines of the lithiumlike aluminum laser is also calculated, and the result indicates that the gain is generated before the establishment of the QSS condition.

DOI: 10.1103/PhysRevE.67.016409 PACS number(s): 52.20.−j, 52.70.−m, 42.55.Vc

## I. INTRODUCTION

Recent advent of high-intensity lasers made it possible for us to generate highly charged ions in high density plasmas, in which ions may be populated in their multiply excited levels, e.g., doubly excited levels. The spectroscopic characterization of such ions and clarification of the production mechanism of doubly excited ions under a given plasma condition are important objectives of the plasma spectroscopy and are necessary for the development of high-brightness x-ray sources such as x-ray lasers. Recently several experimental and theoretical studies relevant to doubly and triply excited ions in dense plasmas have been reported [1–6], in which atomic processes involving multiply excited levels such as resonance excitation (RE) [2] and dielectronic recombination (DR) from excited levels [3,4] are well investigated. Collisional-radiative (CR) models including these processes are constructed and applied to the analysis of spectra from dense plasmas [5,6].

Another kind of atomic process involving doubly excited levels was proposed by Fujimoto and Kato several years ago [7,8]. Figure 1 shows a schematic energy level diagram of ion $z$ and ion $z-1$, where we take heliumlike ions $(z+1)$, lithiumlike ions $(z)$, and berylliumlike ions $(z-1)$ as examples. An excited ion $z$ in the $i-3$ level, for an example, may capture a continuum electron by dielectronic capture process [path (1) in Fig. 1] and become a doubly excited ion $z-1$ in the $(i,j)$ level, where we define the $i$ electron and $j$ electron as the core electron and the spectator electron, respectively. The $(i,j)$ ion may autoionize into another lower level of the $z$ ion [path (2)] or decay to a singly excited $z-1$ ion by emitting a satellite line [path (3)]. The former process is RE and the latter is DR from an excited level. If the electron density is high, instead of these spontaneous processes, collisional excitation and deexcitation between the doubly excited levels may become substantial: in ionizing plasmas a doubly excited ion $(i,j)$ may be excited by the plasma electrons into the next upper level as $(i,j+1)\rightarrow(i,j+2)\rightarrow(i,j+3),\ldots,$ and finally ionized [see path (4)]. This process, $(1)\rightarrow(4)$, is called the dielectronic capture and ladderlike excitation (DL excitation), which enhances the direct excitation rate coefficient from $i$ to $j$ [7,8].

A couple of years ago, the present author showed theoretically [9] and experimentally [10] that the inverse process of DL excitation played a decisive role in a low temperature dense plasma such as a gain medium of a recombining plasma x-ray laser. A $z$ ion in an excited level $i$ may capture a continuum electron by 3-body (3B) or radiative recombination (RR) to form a doubly excited ion $(i,j)$, and subsequent collisional excitation and deexcitation result in substantial populations in the doubly excited levels [see path (5) in Fig. 1]. In low temperature dense recombining plasmas,

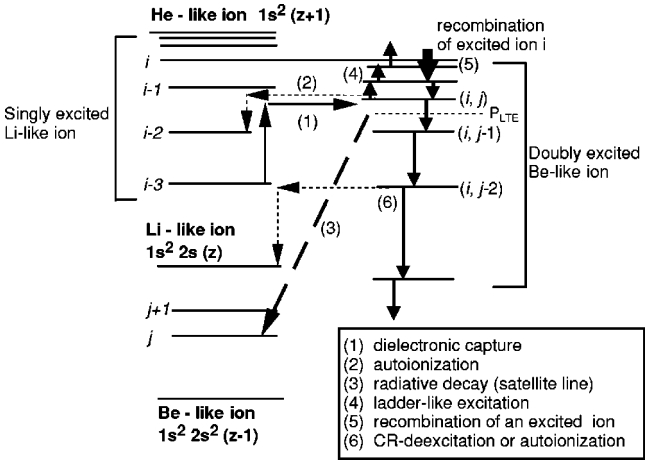


FIG. 1. Schematic energy level diagram of the singly excited Li-like ions, $i,i-1,i-2,\ldots,$ and singly excited Be-like ions, $j,j-1,j-2,\ldots$. The doubly excited levels of the Be-like ions $(i,j)$ hanging below the Li-like excited level $i$ are also shown. Path (1) is dielectronic capture from $i-3$ to the $(i,j)$. Path (2) is autoionization from $(i,j)$ to $i-3$. Path (1) together with path (2) is resonance excitation. Path (3) is the emission process of a satellite line from $(i,j)$ to $j$ (core electron transition). Path (1) together with path (3) is dielectronic recombination from excited ions. Path (4) is ladderlike excitation ionization from the doubly excited levels $(i,j)$. Path (1) together with path (4) is dielectronic capture and ladderlike (DL) excitation. Path (5) is recombination of an excited Li-like ions. Path (6) is collisional-radiative deexcitation of the captured electron $j$.

 

the populations of the doubly excited $(i,j)$ level with $j > p_{LTE}$ may be approximately described by local thermodynamics equilibrium (LTE) with respect to the population of level $i$ and the continuum electron density, where $p_{LTE}$ indicates the lower bound of the LTE region and is determined by the collisional excitation and deexcitation rate and the spontaneous transition probabilities from this level. The doubly excited $(i,j)$ ions may decay in three ways, i.e., autoionization into the lower-lying excited levels of ion $z$ [path (5)→(2) in Fig. 1], the core electron transition [path (5)→(3)], and the spectator electron transition from the LTE region into the lower-lying levels [Path (5)→(6)]. Since the $(i,j)$ level is strongly connected by the collisional processes to the $i$ level of ion $z$ and the continuum electrons, the decrease in the populations of the $(i,j)$ level is compensated rapidly by recombination of ion $z$ in level $i$. Thus these three processes effectively enhance the depopulation of the $i$ level of the $z$ ion.

Including these processes, a CR model for the lithiumlike aluminum ions was performed under quasisteady state (QSS) approximation [9]. The calculated result explained qualitatively the experimental amplification gains of the $3d^2D$-$4f^2F$ and $3d\,^2D$-$5f\,^2F$ lines of the lithiumlike aluminum recombining plasma laser [11–13], whereas without these processes, serious discrepancy between the experiments and calculations [14,15] was found.

In our previous work, since our objective was concerning to the excited level population of singly excited level, a full account of the population kinetics of the doubly excited levels was not clarified. More specifically, first, since the amplification gain of recombining plasma x-ray lasers is generated in a rapidly cooling phase of the plasma, the validity of the QSS approximation has to be discussed. For hydrogen atoms, the temporal development of populations of excited levels and the validity of the QSS approximation have been investigated [16], but a similar study for nonhydrogenic ions including doubly excited levels has not been done to the author's knowledge. Second, the flux of the populations in the doubly excited levels in the ladderlike deexcitation region [see path (6) in Fig. 1] has to be clarified. Our previous result shows that an excited lithiumlike ion in the LTE region recombines with the continuum electron to become a doubly excited berylliumlike ion, which may deexcite due to the collisional-radiative processes into the berylliumlike ground state ion. This series of processes is virtually nothing but the collisional-radiative recombination of the heliumlike ions to the berylliumlike ions without passing through the lithiumlike ground state.

In this paper, we take aluminum ions as an example and construct a CR model involving singly excited lithiumlike ions and singly and doubly excited berylliumlike ions. Since our present objective is to investigate qualitatively the above two points, we adopt a rather simple approximation to estimate atomic processes between the doubly excited levels. In the following we describe the details of our CR model and show the calculation result.

## II. COLLISIONAL-RADIATIVE MODEL

Figure 2 shows the energy level diagram of the CR model

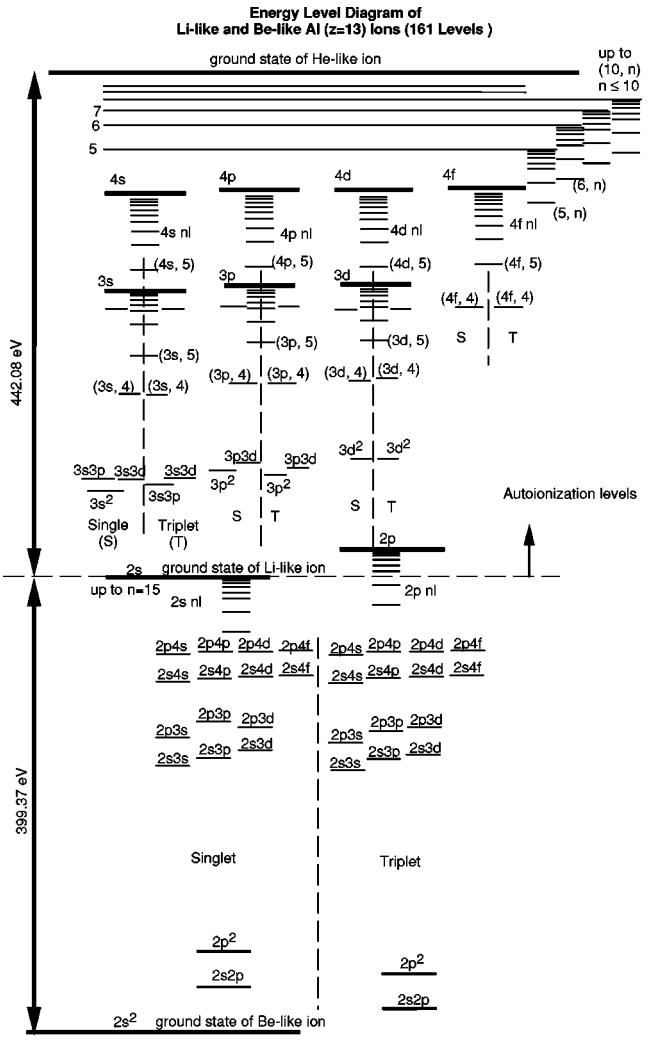


FIG. 2. Energy level diagram of the present CR model.

for the lithiumlike and berylliumlike ions. We take aluminum ions ($z=13$) as an example. $S$ and $T$ represent singlet and triplet, respectively. The temporal development of population $n(p)$ of the level $p$ of ions, lithiumlike and berylliumlike as well, in the plasma can be expressed by the following differential equation:

$$\frac{dn(p)}{dt} = \sum_q C(q,p) n_e n(q) + \left\{ \left[ \sum_{q<p} F(q,p) + \sum_{q>p} C(p,q) \right] n_e + \sum_{q<p} [A(p,q) + A_a(p,q)] \right\} n(p) + \sum_q [F(q,p) n_e + A(q,p) + A_a(q,p)] n(q) - S(p) n_e n(p) + [\alpha(p) n_e + \beta(p) + \gamma(p)] n_e n_{\mathrm{He}}, \tag{1}$$

which is coupled with similar equations for other levels, where $p$ and $q$ represent the singly excited level of the lithiumlike ions or the singly excited level of the berylliumlike

ions or doubly excited levels of the berylliumlike ions. $n_{\mathrm{He}}$ and $n_e$ are the heliumlike ion density and the electron density, respectively. $\alpha(p),\beta(p),\gamma(p)$ are the rate coefficients, respectively, for 3B recombination, RR, and DR from the heliumlike ground state ion to the singly excited level $p$ of the lithiumlike ion. In the case that both levels $p$ and $q$ are lithiumlike ions, or berylliumlike ions, $A(p,q),C(p,q)$, $F(p,q)$ represent Einstein's $A$ coefficient, the collisional excitation rate coefficient, the collisional deexcitation rate coefficients from level $p$ to level $q$, respectively. In the case that level $p$ is a doubly excited berylliumlike ion and level $q$ is a singly excited lithiumlike ion, $A(p,q),A(q,p),C(p,q)$ and $F(q,p)$ are understood to represent autoionization probability from level $p$ to level $q$, dielectronic capture rate coefficient from level $q$ to level $p$, collisional ionization from level $q$ to level $p$, and the sum of the recombination processes (3B and RR) from level $q$ to level $p$, respectively. It is noted that the resonance excitation and dielectronic recombination from excited levels are also treated in the rate equations by using $A(q,p)$ and the following autoionization and spontaneous emission process.

In the following sections, we show the atomic data employed in the present model, where notation $nl$ (or $n$) means the lithiumlike ions $1s^2nl$, and notation $(nl,n'l')$ (or $(n,n')$) means the berylliumlike ions $1s^2nln'l'$ (or $1s^2nn'$).

### A. Singly excited lithiumlike ions

Because the details of the atomic data for the singly excited lithiumlike ions are described in [17], the simplified description is shown for this ion.

For levels with the principal quantum number $n\leqslant 4$, levels with different orbital angular momentum $l$ are treated separately, and levels with $5\leqslant n\leqslant 16$ are assumed to be hydrogenic with the different $l$ levels unresolved. Absorption oscillator strength is given by Lindgard and Nielsen [18], Zhang *et al.* [19], and NSRD data compiled by Wiese *et al.* [20]. Excitation cross section has been calculated by distorted wave approximation for virtually all the transitions between levels ranging from $2s$ to $5g$ by Clark *et al.* [21]. The result is generally in good agreement with those of Zhang *et al.* [19] when the comparison is possible. For ionization cross section of the levels with $n\geqslant 5$, we use calculation by Sampson and co-workers by the infinite $z$ approximation [22–25]. For the RR rate coefficient, we use the calculation by Burgess [26]. Dielectronic recombination rate coefficient is calculated by Bely *et al.* [27] for the lithiumlike oxygen and Vainstein and Safronova calculate the autoionization probability with relativistic effect for $z=6$ through 58 [28]. We follow them and scale the autoionization probability and the radiative decay probability calculated by Bely *et al.* [27].

### B. Singly and doubly excited berylliumlike ions

#### *1. Energy level and Einstein's A coefficient*

The level energies of the $(nl,n'l')$ levels with $n\leqslant 4$ and $n'\leqslant 4$ are calculated using the HULLAC code [29] with the orbital angular momentum and singlet-triplet resolved. Since the output of HULLAC is $j$-$j$ coupling scheme, we recognize the results into the $L$-$S$ coupling scheme. For the triplet levels, the level energies are averaged over the fine-structure sublevels by taking their statistical weights into account. The level energies of the singly excited levels $(2s,n')$ (or $2sn'$) and $(2p,n')$ (or $2pn'$) with $5\leqslant n'\leqslant 10$ are given for the berylliumlike nitrogen in Ref. [30]. We scaled these data to the berylliumlike aluminum ions. For the doubly excited levels $(nl,n')$ with $nl=3s\sim 4f$ and $5\leqslant n'\leqslant 10$ and levels $(n,n')$ with $5\leqslant n\leqslant 10$ and $5\leqslant n'\leqslant 10$, the level energies are derived using hydrogenic approximation together with the level energy of the series limit $1s^2nl$ or $1s^2n$ of the lithiumlike ions where the effective nuclear charge is given by Mayer [31].

Absorption oscillator strength for transitions among the $1s^2nln'l'$ levels with $n\leqslant 4$, $n'\leqslant 4$ are calculated by the HULLAC code. For the other transitions we use the hydrogenic approximation. From these absorption oscillator strengths together with the transition energies we calculate the spontaneous transition probabilities.

#### *2. Electron impact excitation, deexcitation, and ionization*

Collisional excitation and deexcitation cross sections for the transitions among low-lying levels, $2s^2,2s2p,2p^2$, and $2s3l$ levels are calculated by Clark *et al.* [32] for the aluminum ions and Kato *et al.* [33] for the oxygen ions. For other transitions, we evaluate the excitation cross sections from the data of the lithiumlike ions in Ref. [17] as follows: For the core electron transition of $(j,k)\rightarrow(j',k)$, we use the data of the transition of $j\rightarrow j'$ of the lithiumlike ions, and in the same way, the excitation cross section of the spectator electron transition of $(j,k)\rightarrow(j,k')$ is derived from the transition of $k\rightarrow k'$ of the lithiumlike ions. That is,

$$\sigma((j,k),(j',k))=\alpha(z)\times\sigma(j,j')_{\text{Li-like}}, \tag{2}$$

$$\sigma((j,k),(j,k'))=\alpha(z)\times\sigma(k,k')_{\text{Li-like}}, \tag{3}$$

where $\sigma((j,k),(j,k'))$ is the excitation cross section of $(j,k)\rightarrow(j,k')$, and $\sigma(k,k')_{\text{Li-like}}$ is that of $k\rightarrow k'$ of the lithiumlike ions. $\alpha(z)$ is the $z$-scaling factor $[=(z-2)^4/(z-3)^4]$. From these cross sections, the rate coefficients are derived under the assumption that the electron velocity distribution is Maxwellian. Deexcitation rate coefficients are derived from the excitation rate coefficients using the principle of detailed balance.

The ionization rate coefficient for the transition of $(nl,n'l')\rightarrow nl$ with $n'\leqslant 4$ is derived from the ionization rate coefficient of the level $p$ of the singly excited ions [22–25]. For higher-lying levels with $(nl,n')(n'\geqslant 5)$, hydrogenic approximation with effective nuclear charge is employed.

#### *3. Recombination processes*

An ion in an excited level $p$, in the same way as the ground state ion, may capture a continuum electron by the 3BR, RR, and dielectronic capture processes, and become a

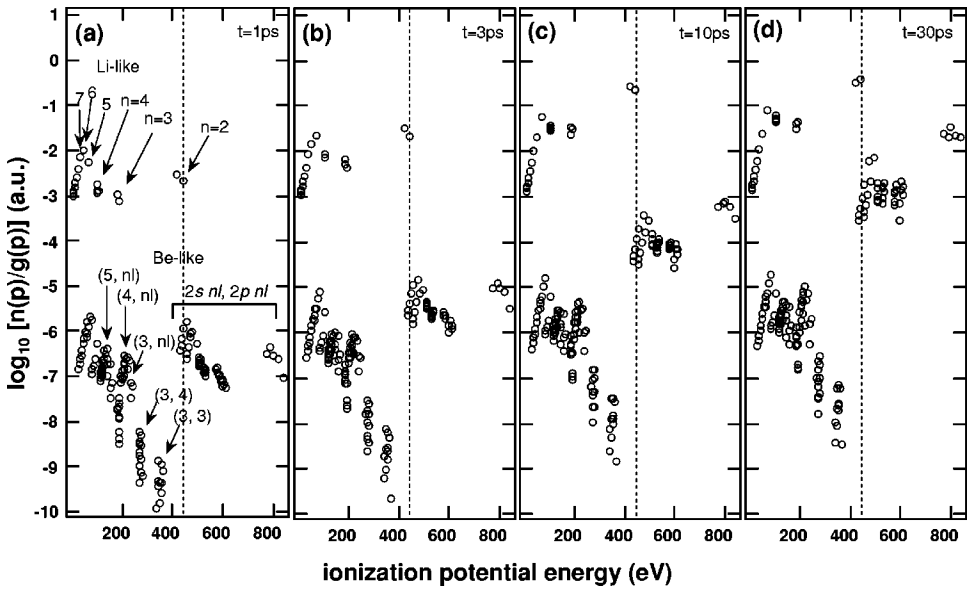


FIG. 3. Temporal evolution of the populations of the Li-like and Be-like excited levels at 1 ps; (a) 3 ps; (b) 10 ps; (c) and 30 ps (d) under the plasma parameter of $n_e=4\times10^{25}$ m$^{-3}$ and $T_e=8$ eV. The time is measured from the start of the recombination. The abscissa is the ionization potential energy, and the ordinate is the relative population of the levels divided by their statistical weights. The arrows indicate the principal quantum numbers or the simplified configurations of the levels. The dotted line represents the ionization potential energy of the Li-like ground state ions.

doubly excited ion. The 3BR and RR rate coefficients for the excited ions are derived from the rate coefficients for the ground state ions as follows:

$$A(j,k)=\alpha(z)\times A(k)_{\text{Li-like}}, \tag{4}$$

where $A(j,k)$ is the 3BR or RR rate coefficient for the doubly excited berylliumlike ions from the lithiumlike excited ion in level $j$, and $A(k)_{\text{Li-like}}$ is the recombination rate coefficient into the level $k$ of the lithiumlike ions. $\alpha(z)$ is a $z$-scaling factor, which is $(z-2)^3/(z-3)^3$ for 3BR and $(z-2)/(z-3)$ for RR.

Autoionization probabilities are given by Moribayashi and Kato [34] for virtually all the transitions from the doubly excited levels of the berylliumlike ions to the $1s^22s$ level of the lithiumlike ions for several ionic species from $z=6$ through 26, and to the $1s^22p$ level for $z=26$ [35]. We scale these data for the present case. Dielectronic capture rate coefficients for these transitions are obtained by using the principle of detailed balance. For other transitions, autoionization probabilities are estimated from the following equation:

$$A_a=\frac{16\pi m\epsilon}{h^3}\frac{g_{z+1}(1)}{g_z(p,nl)}\sigma_d(1\rightarrow p,nl)\,\delta E, \tag{5}$$

where $\sigma_d$ is the dielectronic capture cross section. Since the dielectronic capture cross section across the excitation threshold to the excitation cross section is a continuous function of energy, we estimate the $\sigma_d$ by extrapolation of the excitation cross section of the lithiumlike ions below the excitation threshold.

## III. CALCULATED RESULT AND DISCUSSION

### A. Temporal behavior of excited level populations and validity of the QSS approximation

We start with the heliumlike ground state ions having population $n_{\text{He}}=1$, and recombination starts at $t=0$ s under a plasma condition with the electron temperature $T_e=8$ eV and electron density $n_e=4\times10^{25}$ m$^{-3}$; these plasma parameters are typical in the lithiumlike aluminum recombining plasma laser [10]. Figures 3(a), 3(b), 3(c), and 3(d) show calculated populations of the ground state and the excited levels in the Boltzmann plot at $t=1$ ps, 3 ps, 10 ps, and 30 ps, respectively. The excited levels of the lithiumlike and berylliumlike ions are indicated by arrows. The dotted vertical line is the ionization potential energy of the lithiumlike ground state ions, i.e., the doubly excited levels in the left-hand side are autoionizing levels, and those in the right-hand side are nonautoionizing levels. From Fig. 3(b) to 3(d), the populations of the $(n',nl)$ levels with $n\geqslant3$, i.e., $(3,nl),(3,4),(3,3)$ levels, become smaller as $n$ decreases; this is due to the increase in the autoionization probabilities with the decrease in $n$. Whereas the populations of the $(2s,nl)$ and $(2p,nl)$ levels are large compared with those of the (3, 4) and (3, 3) levels because the $(2p,n)$ with $n\geqslant9$ and $(2s,n)$ levels are nonautoionizing levels.

At $t=1$ ps, the higher-lying excited levels of the lithiumlike ions with $n\geqslant7$ reach their final or LTE values. At $t=3$ ps, the $n=6$ levels of the lithiumlike ions and the higher-lying doubly excited levels of the berylliumlike ions with $(n,n')$ ($n\geqslant6$ and $n'\geqslant6$) reach their final (or LTE in this case) values. This implies that the establishment of the LTE populations in higher-lying doubly excited levels requires at least $\sim3$ ps under the present plasma condition.

The lower-lying levels of the lithiumlike ions with $n \leqslant 5$ and berylliumlike ions with $(5,nl) \sim (2,nl)$ do not reach their QSS populations yet. It takes around $\sim 30$ ps for these levels to reach their QSS populations [see also Figs. 3(c) and 3(d)].

Several years ago, Sawada and Fujimoto discussed the validity of QSS approximation in ionizing and recombining plasmas for hydrogen atoms [16]. In this work, they introduced "response time" $t_{res}$ to describe a time constant in which the excited level populations reach their QSS values, where $t_{res}$ is determined by the inverse of the depopulation rate of Griem's boundary or Byron's boundary [35]. We followed their results, and calculated a response time for the present case. The plasma parameters ($T_e = 8$ eV, $n_e = 4 \times 10^{25}$ m$^{-3}$) and the temporal behaviors of the ions are assumed to scale as $T_e = z_{eff}^2 T_H$, $n_e = z_{eff}^7 n_H$, and $t \propto z_{eff}^{-8} t_H$ in recombining plasmas [36], where $z_{eff}, T_H, n_H$, and $t_H$ are the effective nuclear charge, the equivalent electron temperature, electron density, and time for neutral hydrogen plasma, respectively. The estimated response time for the ions with $z_{eff} = 10$ was $\sim 3 \times 10^{-15}$ s, which is faster by four orders of magnitude than the present result ($3 \times 10^{-11}$ s). This implies that since the lower-lying excited levels of the lithiumlike ions are strongly connected with doubly excited berylliumlike ions, the establishment of the QSS populations in the lower-lying lithiumlike ions is obstructed by the presence of the doubly excited berylliumlike ions until the QSS populations are established in these levels.

In order to show the connection between the lower-lying lithiumlike excited levels and the doubly excited levels of the berylliumlike ions, the population flux from and out of a lithiumlike excited level is investigated. The result is shown in Figs. 4(a) and 4(b). We take the $3d$ excited level as an example. The plasma parameters are the same as those in Fig. 3, and here we assume the QSS condition. In Fig. 4(a), the thick solid line represents deexcitation through doubly excited levels, i.e., sum of the path $(5) \rightarrow (6)$ and path $(5) \rightarrow (2)$ in Fig. 1. The dotted line is collisional deexcitation from the $3d$ to the $3p$ level ($l$-changing), and the thin solid line is collisional-radiative deexcitation from the $3d$ to the $2s$ and $2p$ levels. The thin dashed line is excitation to the upper levels ($n \geqslant 4$) including the contribution of resonance excitation, and the thin chain line is the direct ionization. It is noted that under the present low temperature plasma condition, the contribution from the dielectronic recombination from the $3d$ level is negligibly small.

In the low density region of $n_e < 10^{25}$ m$^{-3}$, the dominant depopulation processes are collisional and radiative deexcitation from the $3d$ level to the $2s$ and the $2p$ levels. As the electron density increases, the $3d$ level is coupled strongly with the doubly excited levels, and for the electron density region of $n_e \geqslant 10^{25}$ m$^{-3}$, the $3d$ level is mainly depopulated through doubly excited levels "hanging" below the $3d$ levels.

Figure 4(b) shows the population flux into the $3d$ level. The thick solid line, thin dotted line, thin solid line, and thin dashed line represent ionization from doubly excited levels hanging below the $3d$ level, $l$-changing, collisional-radiative cascade from upper levels of the lithiumlike ions, and exci-

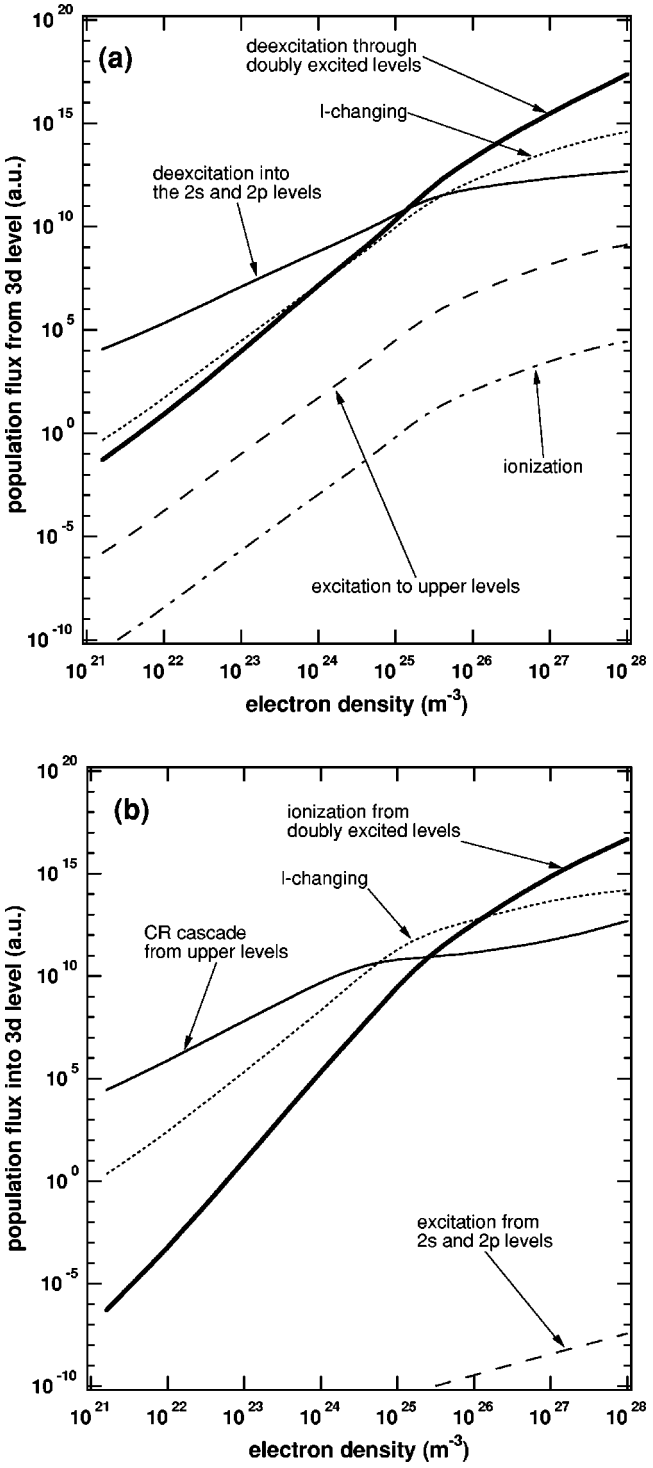


FIG. 4. Population flux out of the $3d$ level of the Li-like ions (a) and flux into the $3d$ level (b). The plasma parameters are the same as those in Fig. 3. We assume the QSS condition. (a) Thick solid line, deexcitation through doubly excited levels; thin solid line, collisional-radiative deexcitation into the lower-lying levels; dotted line, $l$-changing, thin dashed line, excitation into upper-levels; thin chain line, ionization. (b) Thick solid line, ionization from doubly excited levels; thin solid line, collisional-radiative cascade from upper-levels; dotted line, $l$-changing; thin dashed line, excitation from lower-lying levels.

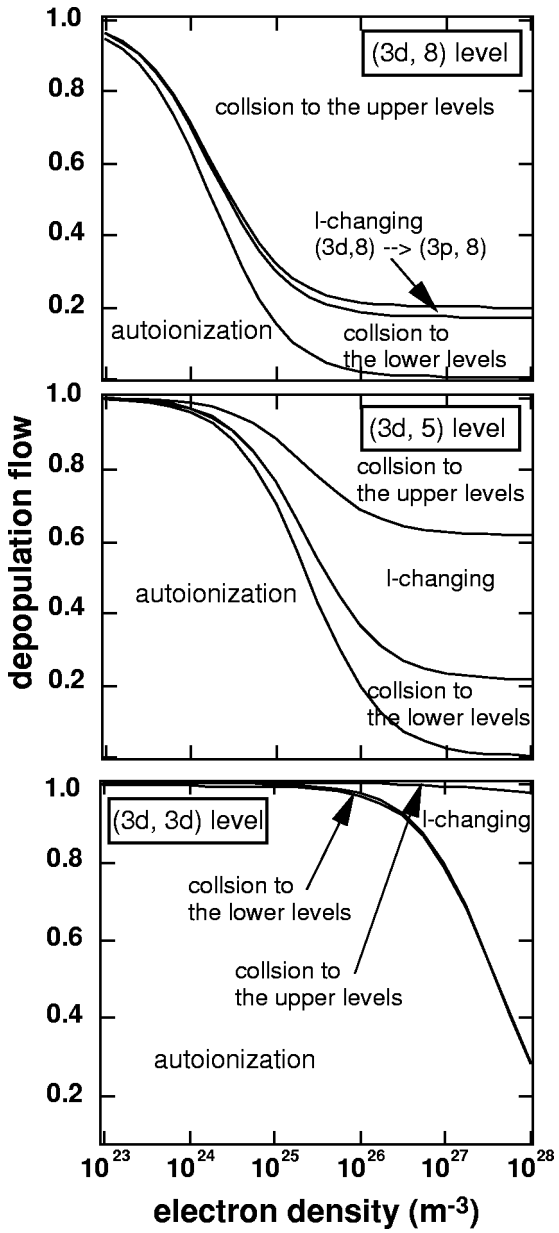


FIG. 5. Electron density dependence of the fraction of the depopulation flow from doubly excited levels of the $(3d,8)$,$(3d,5)$, and $(3d,3d)$ levels.

tation from lower-lying levels of the lithiumlike ions, respectively. Similar to Fig. 4(a), for the electron density of $n_e \geqslant 10^{25}$ m$^{-3}$, the population of the $3d$ level is mainly generated by the ionization from the doubly excited levels.

### B. Population flux in doubly excited levels

In this section we will discuss the depopulation flux in the doubly excited levels. We take the $(3d,8)$, $(3d,5)$, and $(3d,3d)$ levels as examples. The plasma temperature is the same as that in Fig. 3, and QSS condition is assumed. The expected LTE limit of the doubly excited levels is $p_{LTE} \sim 7$ [see Fig. 3(c)], thus the $(3d,8)$ level is in LTE, the $(3d,3d)$ level is out of the LTE region, and the $(3d,5)$ level is in the intermediate region.

Figure 5 shows the population flux out of the $(3d,8)$,$(3d,5)$, and $(3d,3d)$ levels. The ordinate represents the fraction of the depopulation flux from these doubly excited levels, and the total amount is normalized. For the $(3d,8)$ level, in the electron density of $n_e < 10^{24}$ m$^{-3}$, the dominant depopulation process is the autoionization. In $n_e \geqslant 10^{24}$ m$^{-3}$, collisional transitions to the upper and lower levels become substantial, and the contribution from the autoionization becomes small. The $(3d,5)$ level has the same trend in the contribution from the autoionization; however, in $n_e \geqslant 10^{25} \sim 10^{26}$ m$^{-3}$, the collisional downward flow becomes substantial. For the $(3d,3d)$ level, the dominant flow out process is autoionization for almost all the electron density regions. This result, together with Fig. 4(a), leads to the following conclusion: In $n_e \geqslant 10^{26}$ m$^{-3}$, lithiumlike excited ions with $n>3$ capture an electron to form doubly excited ions $(n,n')$ with large $n'(>p_{LTE})$, which depopulate by ladderlike deexcitation into the next lower level $(nl,n'-1) \rightarrow (nl,n'-2) \rightarrow \ldots$. In doubly excited levels $(nl,n')$ with $n' < p_{LTE}$, since the branching ratio of the autoionization becomes large with the decrease in $n'$, finally the doubly excited ions autoionize into lower-lying lithiumlike ions. It is noted that the fraction of the collisional deexcitation from the $(3d,n')$ levels with $n'=3$ to the nonautoionizing level, e.g., $(3d,2l)$ is about 0.02 of that of the autoionization to the low-lying lithiumlike ion under $n_e = 10^{26}$ m$^{-3}$.

In the case of the $(2p,n')$ levels, which is mainly generated by the recombination of the $1s^2 2p$ excited ions, the situation is different. The $(2p,n')$ with $n' \leqslant 9$ are not autoionizing levels, so that the contribution from the autoionization is negligible for this group; rather the ladderlike deexcitation produces berylliumlike ground state ions without passing through the lithiumlike ground state, which suppresses the production of the lithiumlike ground state ions. (See the following section.)

### C. Temporal evolution of amplification gain of the lithiumlike aluminum recombining plasma laser

The temporal evolution of amplification gain of the lithiumlike aluminum recombining laser is calculated. The plasma parameters are assumed to be $T_e = 8$ eV and $n_e = 4 \times 10^{25}$ m$^{-3}$, which are based on the experimental investigation [10,37,38]. We assume pure recombining plasma and that the initial heliumlike ground state density is 0.05 of the electron density at t = 0 ps. Under the present plasma parameters the spectral line broadening is well studied and the linewidths of the $3d\,^2D$-$4f\,^2F$ and $3d\,^2D$-$5f\,^2F$ lines are determined by Stark broadening rather than Doppler broadening [38,39]. We use these experimental data: the line broadening of $3.16 \times 10^{13}$ s$^{-1}$ for the $3d\,^2D$-$4f\,^2F$ line, and $5.96 \times 10^{14}$ s$^{-1}$ for the $3d\,^2D$-$5f\,^2F$ which is dominated by linear Stark broadening.

Figure 6 shows a temporal evolution of the amplification gain coefficients of the $3d\,^2D$-$4f\,^2F$ (thick solid line) and $3d\,^2D$-$5f\,^2F$ (thick dotted line) lines. The calculated gain shows that the peak gain is 8.2 cm$^{-1}$ for the $3d\,^2D$-$4f\,^2F$ line and 4.4 cm$^{-1}$ for the $3d\,^2D$-$5f\,^2F$, which is 1.3$\sim$3 times larger than the experimental gains [12,13,38]. This

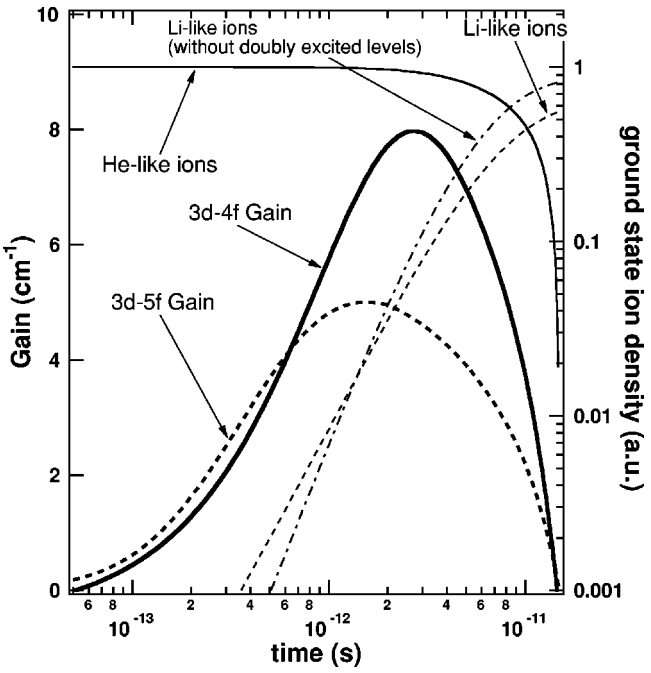


FIG. 6. Temporal behavior of the gain coefficients of the $3d\,^2D$-$4f\,^2F$ (thick solid line) and $3d\,^2D$-$5f\,^2F$ (thick dotted line) lines of the lithiumlike aluminum ions. Thin solid line and thin dotted line are the ground state ion density of the heliumlike and lithiumlike ions, respectively. The thin chain line is the ground state density of the lithiumlike ions in the absence of the doubly excited levels.

may be due to the fact that the experimental gains are time-integrated or due to the overestimation of the heliumlike ground state ion density. Thin solid, thin dotted lines are the heliumlike ground state density, the lithiumlike ground state density, respectively. For a reference, the lithium-like ground state ion density in the absence of contribution from the doubly excited levels is shown by the thin chain line. By including the contribution from the doubly excited levels, the lithiumlike ground state density increases rapidly ($t<1$ ps) whereas the final ion density becomes smaller ($t>2$ ps). This means that in the early time region ($t<1$ ps), the production of the lithiumlike ground state is enhanced by the DL deexcitation [path $(5)\rightarrow(2)$ in Fig. 1] and path $(5)\rightarrow(6)\rightarrow(2)$, whereas in the later time region ($t>2$ ps), substantial populations are generated in the $2p$ level, and the recombination flux of the $2p$ level to the $(2p,nl)$ levels suppresses the production of the lithiumlike ground state density.

The peak gains of both the lasing lines in Fig. 6 are obtained around $2\sim3$ ps from the start of the recombination. Since Fig. 3 indicates that the populations of the $n=3,4$, and 5 levels of the lithiumlike ions are not in their QSS values at 3 ps, we can conclude that the QSS treatment for the amplification gain is not valid for the present case.

The gain duration of $\sim10$ ps of both the lasing lines is determined by the recombination time of the heliumlike ground state ions. In actual experiments using laser-produced plasmas, the heliumlike ground state ions are produced in high temperature and high density region and flow out due to the density gradient into the observation area continually. This may lead to elongation of experimental gain duration, which may be determined by hydrodynamics motion of the heliumlike ions. In order to treat it, we need to develop an integrated code, in which temporal evolution of electron density, temperature, ion abundance, and the excited level populations are treated simultaneously. Development of this kind of simulation code is an important objective; however, it is not the scope of this paper.

## IV. SUMMARY

We have constructed a CR model for the lithiumlike and berylliumlike aluminum ions. In this model, we have treated virtually all the doubly excited levels of the berylliumlike ions and investigated the effect of these ions on the population kinetics of the singly excited lithiumlike ions. The calculated result shows that the ''response time'' of lower-lying lithiumlike excited levels becomes much larger by the presence of the doubly excited levels, and the production rate of the lithiumlike ground state ions is affected by the CR recombination of the $2p$ excited level. Temporal evolution of amplification gains of the lithiumlike aluminum x-ray laser shows that the QSS approximation is not valid for the lasing condition.

## ACKNOWLEDGMENTS

The author acknowledges support from Dr. Akira Sasaki in JAERI for the calculations using the HULLAC code, and thanks Professor Takashi Fujimoto of Kyoto University for his comments, criticism, and encouragement.

[1] Papers relevant to multiple-excited ions in plasma can be seen in J. Quant. Spectros. Radiat. Transf. **58** (4-6) 1997; **65** (1-3) (2000); **71** (2-6) (2001).
[2] K.B. Fournier, W.H. Goldstein, M. May, M. Finkenthal, and J.L. Terry, Phys. Rev. A **53**, 3110 (1996).
[3] F.B. Rosmej, B.A. Brynetkin, A.Ya. Faenov, Y. Skobelev, M.P. Kalashnikov, P.V. Nickels, and M. Schnurer, J. Phys. B **29**, L299 (1996).
[4] F.B. Rosmej, A.Ya. Faenov, T.A. Pikuz, F. Flora, P.Di. Lazzaro, T. Letardi, A. Grilli, A. Reale, L. Palladino, G. Tomassetti, A. Scafati, and L. Reale, J. Phys. B **31**, L921 (1998).
[5] R. Doron, E. Behar, M. Fraenkel, P. Mandelbaum, A. Zigler, J.L. Schwob, A.Ya. Faenov, and T.A. Pikuz, Phys. Rev. A **58**, 1859 (1998).
[6] R.C. Mancini, A.S. Shlyaptseva, P. Audebert, J.P. Geindre, S. Bastiani, J.C. Gauthier, G. Grillon, A. Mysyrowicz, and A. Antonetti, Phys. Rev. E **54**, 4147 (1996).
[7] T. Fujimoto and T. Kato, Phys. Rev. Lett. **48**, 1022 (1982).
[8] T. Fujimoto and T. Kato, Phys. Rev. A **32**, 1663 (1985).
[9] T. Kawachi and T. Fujimoto, Phys. Rev. E **55**, 1836 (1997).

[10] T. Kawachi, K. Ando, C. Fujikawa, H. Oyama, N. Yamaguchi, T. Hara, and Y. Aoyagi, J. Phys. B **33**, 156 (1999).
[11] T. Kawachi, K. Ando, Y. Aoyagi, M. Aoyama, T. Hara, and A. Sasaki, J. Opt. Soc. Am. B **14**, 1863 (1997).
[12] A. Carillon, M.J. Edwards, M. Grande, M.J.de C. Henshaw, P. Jaegle, G. Jamelot, M.H. Key, G.P. Kiehn, A. Klisnick, C.L.S. Lewis, D. O'Neill, G.J. Pert, S.A. Pamsden, C.M.E. Regan, S.J. Rose, R. Smith, and O. Willi, J. Phys. B **23**, 147 (1990).
[13] T. Hara, K. Ando, N. Kusakabe, H. Yashiro, and Y. Aoyagi, Jpn. J. Appl. Phys., Part 2 **28**, L1010 (1989).
[14] A. Klisnick, A. Sureau, H. Guennou, C. Moller, and J. Virmont, Appl. Phys. B: Photophys. Laser Chem. **B50**, 153 (1990).
[15] T. Kawachi and T. Fujimoto, Phys. Rev. E **51**, 1440 (1995).
[16] K. Sawada and T. Fujimoto, Phys. Rev. E **49**, 5565 (1994).
[17] T. Kawachi, T. Fujimoto, and G. Csanak, Phys. Rev. E **51**, 1428 (1995).
[18] A. Lindgard and S.E. Nielsen, At. Data Nucl. Data Tables **19**, 533 (1977).
[19] H.L. Zhang, D.H. Sampson, and C.J. Fontes, At. Data Nucl. Data Tables **44**, 31 (1990).
[20] W.L. Wiese, M.W. Smith, and B.M. Glennon, NSRD-NBS 4, 1966 (unpublished).
[21] R.E.H. Clark, G. Csanak, and J. Abdallah, Jr., Phys. Rev. A **44**, 2874 (1991).
[22] L.B. Golden and D.H. Sampson, J. Phys. B **10**, 2229 (1977).
[23] L.B. Golden, D.H. Sampson, and K. Omidvar, J. Phys. B **11**, 3235 (1978).
[24] L.B. Golden and D.H. Sampson, J. Phys. B **13**, 2645 (1980).
[25] R.E.H. Clark and D.H. Sampson, J. Phys. B **17**, 3311 (1984).
[26] A. Burgess, Mem. R. Astron. Soc. **69**, 1 (1964).
[27] F. Bely-Dubau, J. Dubau, P. Faucher, and L. Steenman-Clark, J. Phys. B **14**, 3313 (1981).
[28] L.A. Vainstein and U.I. Safronova, At. Data Nucl. Data Tables **21**, 49 (1978).
[29] M. Klapisch and A. Bar-Shalom, J. Quant. Spectrosc. Radiat. Transf. **58**, 687 (1997).
[30] W.L. Wiese, J.R. Fuhr, and T.M. Deters, *Atomic Transition Probabilities of Carbon, Nitrogen, and Oxygen. A Critical Data Compilation*, J. Phys. and Chem. Ref. Data Monograph No. 7 (ACS and AIP, New York, 1996).
[31] H. Mayer, Los Alamos Scientific Laboratory Report, No. LA-607, 1947 (unpublished).
[32] R.E.H. Clark, N.H. Magee, J.B. Mann, and A.L. Merts, Astrophys. J. **254**, 412 (1982).
[33] T. Kato, J. Lang, and K.A. Berrington, At. Data Nucl. Data Tables **44**, 133 (1990).
[34] K. Moribayashi and T. Kato, NIFS-DATA-41, 1997 (unpublished).
[35] K. Moribayashi and T. Kato, NIFS-DATA-36, 1996 (unpublished).
[36] S. Byron, R.C. Stabler, and P. Bortz, Phys. Rev. Lett. **8**, 376 (1967).
[37] T. Fujimoto, J. Phys. Soc. Jpn. **54**, 2905 (1980).
[38] J.C. Moreno, H.R. Griem, S. Goldsmith, and J. Knauer, Phys. Rev. A **39**, 6033 (1989).
[39] H.R. Griem, *Principle of Plasma Spectroscopy* (Cambridge University Press, Cambridge, 1977).